

# Hydrophobic ion interaction on $\text{Na}^+$ activation and dephosphorylation of reconstituted $\text{Na}^+, \text{K}^+$ -ATPase

Flemming Cornelius \*

*Institute of Biophysics, University of Aarhus, Ole Worms Alle 185, DK-8000 Aarhus, Denmark*

Received 6 December 1994; accepted 16 December 1994

## Abstract

In liposomes with reconstituted shark  $\text{Na}^+, \text{K}^+$ -ATPase an uncoupled  $\text{Na}^+$ -efflux and a  $\text{Na}^+/\text{Na}^+$  exchange can be induced on inside-out oriented pumps by the addition of external (cytoplasmic)  $\text{Na}^+$  and MgATP to liposomes that either do not contain  $\text{Na}^+$  (and other alkali cations), or include 130 mM  $\text{Na}^+$  internally (extracellular). Both modes of exchange are electrogenic and accompanied by a net hydrolysis of ATP. The coupling ratio of positive net charges translocated per ATP split is found to be close to 3:1 and 1:1, respectively, for the two modes of exchange reactions at pH 7.0. By addition of the hydrophobic anion tetraphenylboron ( $\text{TPB}^-$ ), which imposes a negative electrostatic membrane potential inside the lipid bilayer, the ATP hydrolysis accompanying uncoupled  $\text{Na}^+$  efflux is increased with increasing  $\text{TPB}^-$  concentrations. Cholesterol which increases the inner positive dipole potential of the bilayer counteracted this activation by  $\text{TPB}^-$  of uncoupled  $\text{Na}^+$  efflux. Using the structural analog tetraphenylphosphonium ( $\text{TPP}^+$ ), which elicits an inside positive membrane potential, ATP hydrolysis accompanying uncoupled  $\text{Na}^+$ -efflux is decreased. The rate of dephosphorylation in the absence of extracellular alkali cations was affected in a similar manner, whereas the dephosphorylation in the presence of extracellular  $\text{Na}^+$  inducing  $\text{Na}^+/\text{Na}^+$  exchange was unaffected by the hydrophobic ions. In both modes of exchange the phosphorylation reaction was independent of the presence of hydrophobic ions. The hydrophobic ions affected the apparent affinity for cytoplasmic  $\text{Na}^+$ , indicating that binding of cytoplasmic  $\text{Na}^+$  may involve the migration of cations to binding sites through a shallow cytoplasmic access channel. The results are in accordance with the simple electrostatic model for charge translocation in which two negative charges in the cytoplasmic binding domain of the  $\text{Na}^+, \text{K}^+$ -ATPase co-migrate during cation transport.

**Keywords:** Electrogenic transport; ATPase,  $\text{Na}^+/\text{K}^+$ -; Reconstitution; Uncoupled sodium ion efflux; Sodium–sodium ion exchange; Hydrophobic ion; Dephosphorylation; Membrane potential

## 1. Introduction

In the absence of extracellular  $\text{Na}^+$  and  $\text{K}^+$  the  $\text{Na}^+, \text{K}^+$ -ATPase catalyses an ATP supported  $\text{Na}^+$  extrusion [1–3] known as the uncoupled  $\text{Na}^+$ -efflux, or  $\text{Na}^+/\text{O}$  exchange. In the absence of  $\text{K}^+$  extracellular  $\text{Na}^+$  can act as a (poor)  $\text{K}^+$ -substitute and the sodium-pump engages in a so-called ATP driven  $\text{Na}^+/\text{Na}^+$  exchange [4–6]. Both modes of exchange are electrogenic and accompanied by a net charge movement [6–8]. In the Albers-Post kinetic scheme [9,10], used here as a frame of reference, both the  $\text{Na}^+/\text{O}$  exchange and the  $\text{Na}^+/\text{Na}^+$  exchange take place by a consecutive (ping-pong) reaction in which 3 cytoplasmic  $\text{Na}^+$  bind to an  $\text{E}_1\text{ATP}$ -form of the enzyme ( $\text{E}_1\text{A}$  in Fig. 1). As a result of a phosphorylation of the enzyme the

3  $\text{Na}^+$  ions are occluded and translocated across the membrane by a subsequent deocclusion. This ‘sodium-limb’ of the cycle is associated with transfer of electrical net charge [11–14], in which the deocclusion and release of  $\text{Na}^+$  to the extracellular side through a narrow access channel, an ion well [15], is believed to constitute the major charge translocating steps [14,16–19]. Following a dephosphorylation the enzyme returns to an  $\text{E}_2$ -form either with no alkali cations bound ( $\text{Na}^+/\text{O}$  exchange), or after binding of extracellular  $\text{K}^+$ , or its congeners (as, e.g.,  $\text{Na}^+$  in  $\text{Na}^+/\text{Na}^+$  exchange). In this ‘potassium-limb’ of the cycle only the binding and release of extracellular cations and possibly their subsequent occlusion are believed to be electrogenic, probably due to their passage through an extracellular ion-well to arrive at their binding sites [20–22], whereas the ion translocation and associated conformational changes are presumably electroneutral. The electroneutral ADP-activated  $\text{Na}^+/\text{Na}^+$  exchange which takes

\* Corresponding author. Fax: +45 86 129599.

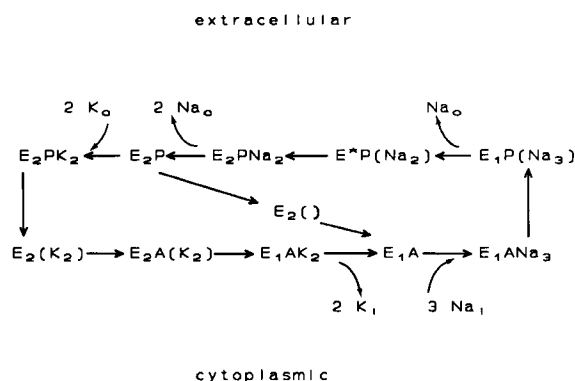


Fig. 1. Simplified scheme for the Na<sup>+</sup>/K<sup>+</sup> exchange reactions based on the Albers-Post model [9,10], and the modifications introduced by Karlisch et al. [64], Nørby et al. [65], Yoda and Yoda [66], and Cornelius and Skou [6]. The scheme depicts the two enzyme conformations E<sub>1</sub> (the Na<sup>+</sup>-form) and E<sub>2</sub> (the K<sup>+</sup>-form) and their phosphorylated and occluded forms. For clarity the addition of ATP (ligand A) and the release of P<sub>i</sub> and ADP have been omitted. The Na<sup>+</sup>/Na<sup>+</sup> exchange is believed to take place via the same pathway as for the physiological Na<sup>+</sup>/K<sup>+</sup> exchange, but with extracellular Na<sup>+</sup> substituting for K<sup>+</sup>. The uncoupled Na<sup>+</sup> efflux can take place by a dephosphorylation of 'empty' E<sub>2</sub>P. It is unknown if an enzyme species equivalent to an occluded form is formed by the dephosphorylation of E<sub>2</sub>P (E<sub>2</sub>(<sup>0</sup>)). Regarding the translocation of charges, a model is assumed where the cytoplasmic binding domain of the Na<sup>+</sup>-pump contains two negatively charged mobile groups that compensate two of the three charges when the 3 cytoplasmic Na<sup>+</sup> bind, so that only one positive net charge is translocated in the sodium-limb (right-hand part) of the scheme. In the case of electrogenic Na<sup>+</sup>/Na<sup>+</sup> exchange the returning from the extracellular side is believed to be electroneutral, and the two negative charges move in concert with the two extracellular Na<sup>+</sup>, whereas in the case of uncoupled Na<sup>+</sup> efflux the two negative charges return uncompensated.

place by a shuttling back and forth via the Na<sup>+</sup>-limb in the Albers-Post scheme, is absent in the shark Na<sup>+</sup>,K<sup>+</sup>-ATPase [6] probably due to the strongly poised equilibrium towards the E<sub>2</sub>P-form of phosphoforms in this preparation.

In order to account for the electroneutral K<sup>+</sup> translocation in the physiological Na<sup>+</sup>:K<sup>+</sup> exchange, and for the lack of a negative slope in the *I*-*V* curves in several cell types including heart muscle and squid axon [12,23,24], a simple electrostatic model for the charge translocation has been suggested in which the cytoplasmic ligand binding domain, which normally binds 3 Na<sup>+</sup>, encloses two negative charges [12,25], that co-migrate with the ligands during turnover. In the sodium-limb one positive net-charge is therefore translocated, whereas in the potassium-limb the two positive charges from the two K<sup>+</sup> ions are neutralized. For this to be true the two negative charges in the binding domain must apparently return uncompensated during Na<sup>+</sup>/0 exchange, making this pathway electrogenic. Whether or not the K<sup>+</sup>-translocating pathway does include charge movement is still controversial, and to demonstrate it may depend on the establishment of suitable experimental conditions, especially non-saturating extracellular K<sup>+</sup>-concentrations [22].

In the present study the electrogenic nature of the potassium-limb in the Albers-Post scheme is investigated

on inside out reconstituted shark Na<sup>+</sup>,K<sup>+</sup>-ATPase [26] by comparing both the turnover rate of hydrolysis at varying cytoplasmic and extracellular Na<sup>+</sup>-concentrations, and the rate of spontaneous dephosphorylation accompanying the two transport modes Na<sup>+</sup>/Na<sup>+</sup> exchange and Na<sup>+</sup>/0 exchange under conditions where the intramembranous potential barrier is perturbed by addition of the hydrophobic (lipophilic) ions tetraphenylboron (TPB<sup>-</sup>) and tetraphenylphosphonium (TPP<sup>+</sup>).

## 2. Methods

In the present experiments liposomes with incorporated shark Na<sup>+</sup>,K<sup>+</sup>-ATPase were used. The preparation of proteoliposomes, determination of the orientation of inserted Na<sup>+</sup>,K<sup>+</sup>-ATPase and the measurements of specific hydrolytic activity were performed as previously described by Cornelius and Skou [26]. The lipid composition of the liposomes was phosphatidylcholine (PC)/phosphatidylethanolamine (PE)/phosphatidylinositol (PI)/cholesterol (chol) = 48:12:2:38 (mol fractions). In experiments where cholesterol was omitted the proportions of the phospholipids, and the lipid to protein weight ratio were retained. Proteoliposomes were prepared in two media: Na<sup>+</sup>-free, sucrose-media where the liposomes contained sucrose (260 mM), MgCl<sub>2</sub> (2 mM) and histidine (30 mM, pH 7.0), or Na<sup>+</sup>-media in which the liposomes contained NaCl inside in varying concentrations by isosmotic replacement of the sucrose. The sucrose-vesicles were used to study the hydrolytic activity and the dephosphorylation associated with the uptake of external Na<sup>+</sup> in the absence of internal alkali cations during the so called uncoupled Na<sup>+</sup> efflux (Na<sup>+</sup>/0 exchange). The Na<sup>+</sup>-vesicles were used to investigate the ATP driven Na<sup>+</sup>/Na<sup>+</sup> exchange. The expressions 'efflux' and 'influx' refer to the cellular situation and are therefore equivalent to uptake and extrusion in the proteoliposomes, respectively, due to activation of exclusively inside:out-oriented (i:o) enzyme molecules. In the same way the external side or medium corresponds to the original cytoplasmic side, and the internal side to the original extracellular side of the enzyme. The time used to allow measurements of either hydrolysis or potential in the case of Na<sup>+</sup>/0 exchange was kept small enough to prevent an increase in intravesicular Na<sup>+</sup> in sufficient concentrations to activate ATP-driven Na<sup>+</sup>/Na<sup>+</sup> exchange. The rate of ATP-hydrolysis on i:o oriented Na<sup>+</sup>,K<sup>+</sup>-ATPase was measured using [<sup>32</sup>P]ATP employing the method of Lindberg and Ernster [27]. In measurements of maximum hydrolytic capacity of inside-out Na<sup>+</sup>,K<sup>+</sup>-ATPase, the proteoliposomes were preincubated with Mg<sup>2+</sup> (5 mM), P<sub>i</sub> (1 mM) and ouabain (1 mM) in order to inhibit ATP-hydrolysis due to enzyme reconstituted with both sides exposed (n-o oriented, see Cornelius and Skou [26]) and Mg<sup>2+</sup> and P<sub>i</sub> were then subsequently diluted 5-fold in the test medium

(also containing 1 mM ouabain) to avoid inhibition from inorganic phosphate.

The steady-state level of phosphorylation as well as the rate of dephosphorylation of reconstituted inside-out oriented enzyme in the absence of  $K^+$  (spontaneous dephosphorylation) were measured at 10°C as follows. Firstly, non-oriented enzyme molecules were inactivated by preincubating with ouabain,  $Mg^{2+}$ , and  $P_i$  as described above. If  $Na^+$ -vesicles with high  $[Na^+]$  were used, the external  $Na^+$  concentration was lowered to below 30 mM by centrifugation of the proteoliposomes through a Sephadex

G-50 column as described by Penefsky [28], otherwise the ouabain inhibition was incomplete. Secondly, the i:o enzyme was treated with 10  $\mu M$  [ $^{32}P$ ]ATP for 6 s in the same medium after adjusting to 65 mM  $Na^+$ . The inhibition by ouabain of phosphorylation on non-oriented enzyme is complete under these conditions as controlled with unisided membrane bound enzyme, or with reconstituted enzyme after permeabilizing the proteoliposomes with the detergent  $C_{12}E_8$ .

The maximum level of phosphorylation was determined by adding an equal volume of a stopping solution at 0°C

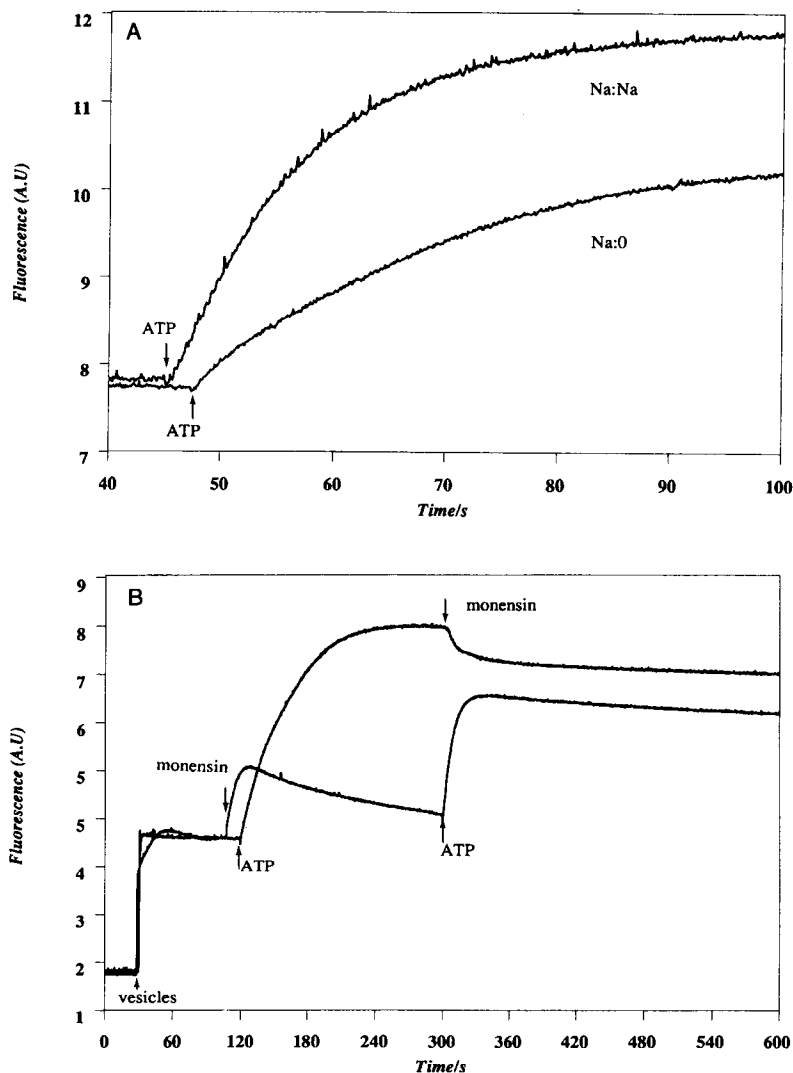


Fig. 2. Time-course of the membrane-potential dependent fluorescence of oxonol VI in the presence and absence of extracellular  $Na^+$ . The oxonol VI response to transmembrane potential development (inside positive) when reconstituted inside-out sodium-pumps are activated by the addition of 100  $\mu M$  ATP in either uncoupled  $Na^+$  efflux (no internal  $Na^+$ ), or in the presence of 117 mM internal (extracellular)  $Na^+$ . Excitation wavelength is 580 nm and a cut-off filter of 660 nm is used on the emission side. The concentration of oxonol VI is 540 nM, and 75  $\mu l$  proteoliposomes are added to the cuvette containing 2 ml 117 mM  $Na^+$ , 26 mM sucrose, 2 mM  $Mg^{2+}$ , 30 mM histidine pH 7.0 (20°C). In panel A the two fluorescence responses are from two different batches of proteoliposomes prepared in the presence (upper trace, Na/Na), or absence of  $Na^+$  (lower trace, Na/0). In panel B the upper trace is the oxonol response due to activation by ATP of reconstituted sodium-pumps in proteoliposomes without internal  $Na^+$ . The subsequent addition of monensin produces a drop in transmembrane potential due to increased bilayer conductance. The lower trace shows the same liposomes equilibrated with external  $Na^+$  (117 mM) by addition of monensin. At the first addition of monensin (722 nM) an inside positive diffusion potential first develops due to the  $Na^+$  gradient; as  $Na^+/H^+$  exchange proceeds, the gradients disappear and the potential vanishes. The subsequent addition of ATP elicits a potential response due to activation of  $Na^+/Na^+$  exchange. Fluorescence is given in arbitrary units and from calibration curves, using different  $K^+$ -gradients clamped with valinomycin to generate known Nernst potentials, the maximum transmembrane potentials are calculated to be about 200 mV.

containing 10% trichloroacetic acid (TCA), 100 mM phosphoric acid and 20% glycerol, followed by protein precipitation with 0.15% sodium desoxycholate (DOC). In the determination of dephosphorylation rate the stopping solution was added at different ageing times by chasing of radioactive ATP by 1 mM unlabeled ATP and 10 mM  $\text{Mg}^{2+}$ . The high  $\text{Mg}^{2+}$  concentration is necessary presumably in order to decrease the concentration of free ATP, which otherwise substantially slowed down the dephosphorylation in this preparation. The same effect of  $\text{Mg}^{2+}$  was originally observed in membrane preparations from shark  $\text{Na}^+, \text{K}^+$ -ATPase by Skou (personal communication). The precipitate was washed twice with ice cold washing solution containing 0.1% TCA, 10 mM phosphoric acid and 10 mM sodium pyrophosphate. Protein [29] and radioactivity were determined after resuspension in 1 M NaOH at 55°C.

The transmembrane potential ( $V_m$ ) in proteoliposomes was measured using the fluorochrome oxonol VI essentially as described by Apell and Bersch [30]. The stoichiometry of net charges translocated per ATP hydrolysed was calculated from the current ( $I$ ) generated by the  $\text{Na}^+$ -pump measuring the initial rate of development of membrane potential ( $dV_m/dt$ ):  $I = C_m A_m (dV_m/dt)/e$ , as previously described in detail [3,7]. A specific capacitance of the bilayer of  $1 \mu\text{F}/\text{cm}^2$  is assumed [31] and a mean diameter of the proteoliposomes of 220 nm, as measured with dynamic laser light scattering (Nicom, US), is used to calculate the surface area ( $A_m$ ).  $e$  is the elementary charge. The fluorescence signal from oxonol VI after excitation at 580 nm was measured at emission wavelengths  $> 660$  nm using a Spex spectrofluorimeter. The data were collected and analyzed on an IBM PS/2 computer.

$\text{TPP}^+$  was obtained from Aldrich,  $\text{TPB}^-$  from Sigma, and DOC from Merck. All reagents were freshly prepared before use.

### 3. Results

The maximum hydrolytic activity of reconstituted inside-out  $\text{Na}^+, \text{K}^+$ -ATPase accompanying uncoupled  $\text{Na}^+$ -efflux with 260 mM sucrose inside the proteoliposomes and 130 mM NaCl outside ( $\text{Mg}^{2+}$  1 mM,  $\text{P}_i$  0.2 mM, ATP 25  $\mu\text{M}$ , histidine 30 mM pH 7.0) was  $55.6 \pm 0.3 \mu\text{mol}/\text{mg}$  per h (mean  $\pm$  S.D.,  $n = 6$ ) at 20°C. The hydrolytic activity associated with  $\text{Na}^+/\text{Na}^+$  exchange where internal sucrose was replaced with 130 mM NaCl but under otherwise identical conditions was  $197.3 \pm 1.3 \mu\text{mol}/\text{mg}$  per h (mean  $\pm$  S.D.,  $n = 6$ ) at 20°C (this value often varied considerably for different preparations for unknown reasons).

#### 3.1. Stoichiometry of exchange reactions

With the two proteoliposome preparations ( $\pm$  internal  $\text{Na}^+$ ) the maximum turnover rate of net charges translo-

cated per ATP split was  $2.80 \pm 0.10$  for uncoupled  $\text{Na}^+$  efflux and  $1.10 \pm 0.06$  (mean  $\pm$  S.D.,  $n = 3$ ) for  $\text{Na}^+/\text{Na}^+$  exchange, in accord with previous reports [7,8,32]. These figures were obtained from measurements of initial rate of transmembrane potential development ( $dV_m/dt$ ) using the potential sensitive fluorescent oxonol VI as described in Methods. The oxonol responses illustrated in Fig. 2 were obtained at saturating cytoplasmic  $\text{Na}^+$  and in the absence of internal  $\text{Na}^+$  for uncoupled  $\text{Na}^+$  efflux. In  $\text{Na}^+/\text{Na}^+$  exchange, the proteoliposomes were either prepared in the presence of  $\text{Na}^+$ , or, to facilitate direct comparison, liposomes without internal  $\text{Na}^+$  were equilibrated with external  $\text{Na}^+$  by addition of the  $\text{Na}^+$  ionophore monensin. As indicated, the addition of monensin initiated an internal positive transmembrane potential due to the  $\text{Na}^+$  gradient, which then gradually declined as the liposomes equilibrated with  $\text{Na}^+$ .

#### 3.2. $\text{TPB}^-$ and $\text{TPP}^+$ binding to bilayers

Partition coefficients for  $\text{TPB}^-$  and  $\text{TPP}^+$  lie in the range of  $2 \cdot 10^5$  nm and 40 nm, respectively [33,34]. The much larger partition coefficient for the negative hydrophobic ion is a generally found property which is explained by the existence of an positive inner dipole potential [35]. From the partition coefficients and with the amount of proteoliposomes used in the assays a free concentration of 1  $\mu\text{M}$   $\text{TPB}^-$  corresponds to 1 adsorbed molecule  $\text{TPB}^-$  per 240 phospholipids (PL), which is well below the expected concentration ratio of 1:100  $\text{TPB}^-/\text{PL}$  where saturation behaviour due to limiting space charge is observed [34], compare Fig. 4. For  $\text{TPP}^+$  the 100  $\mu\text{M}$  corresponds to 1:1200  $\text{TPP}^+/\text{PL}$ .

#### 3.3. Potential effects of hydrophobic ions

Addition of hydrophobic ions to proteoliposomes induces intramembraneous electrostatic potentials, due to their partitioning into the hydrocarbon region of the bilayer leaving their counterions at the membrane surfaces. The location, charge density, and potential profiles can be predicted from calculated free energy of interaction including the electrical Born-Image- and dipole terms as well as the non-electrical hydrophobic interaction terms. Detailed description of the hydrophobic ion interaction with lipid bilayers has been previously given by Ketterer et al. [36], Andersen et al. [33], Honig et al. [37], and Flewelling and Hubbell [34,35]. The calculated profile and magnitude of the electrostatic membrane potentials created by hydrophobic ions are model dependent. Using a discrete charge model with a simple rigid lattice for the adsorbed hydrophobic ions and their counterions Mauzerall and Drain [38] calculated a maximum membrane potential for  $\text{TPB}^-$  in 100 mM NaCl at a  $\text{TPB}^-$  charge density of  $0.05 \text{ nm}^{-2}$  to be  $-70$  mV in the centre of the bilayer, assuming the membrane dielectric decaying exponentially from 80 in the

water phase to 3 in the bilayer centre. The adsorption plane for the hydrophobic ions was placed  $\sim 2$  nm inside a 8 nm bilayer. It is necessary to take into consideration effects of the discrete charges, as opposed to a smeared charge, since in the former the membrane potential varies also outside the space enclosed by the charge lattices (Fig. 3).

In Fig. 3A hypothetical steady-state potential profiles for  $\text{TPP}^+$  and  $\text{TPB}^-$  are depicted. Since  $\text{TPB}^-$  or  $\text{TPP}^+$  is added to the outside of the proteoliposomes, transmembrane potentials ( $V_m$ ) as well as internal membrane potentials will initially be present, since the hydrophobic ions

added are lipid permeable whereas their counterions ( $\text{Cl}^-$ ,  $\text{Na}^+$ ) are much less so. Therefore, in addition to the internal membrane potentials (negative inside the bilayer for  $\text{TPB}^-$  and positive for  $\text{TPP}^+$ )  $\text{TPB}^-$  produces an inside negative transmembrane potential, and  $\text{TPP}^+$  an inside positive transmembrane potential, exactly as the equilibrium potentials which can be imposed by the use of lipophilic ion-carrier complexes such as valinomycin/ $\text{K}^+$ . However, lipophilic ions with very high partition coefficients have very low free concentrations in the medium and their effectiveness in the creation of transmembrane potentials will be accordingly small [33,40]. Although the profile of membrane potentials will initially be asymmetric, it will quickly become symmetric (within 1 min for  $\text{TPB}^-$  [41]), since the diffusion of the hydrophobic ions in the bilayer is high especially for  $\text{TPB}^-$  [34,41]. In order to distinguish between the effects of the two potentials (internal vs. transmembrane), several controls were conducted in which transmembrane potentials were abolished: (i) experiments where the transmembrane potential was clamped to zero by the use of monensin in the presence of an equal concentration of  $\text{Na}^+$  on either side of the bilayer, (ii) proteoliposomes were used which were prepared in the presence of the hydrophobic ions (symmetric case with no transmembrane potential), and finally (iii) unsided preparations were employed. All controls indicate that the effects from putative transmembrane potentials are negligible, as expected.

The presence of internal membrane potentials can be detected in membrane fragments by the potential sensitive fluorochrome RH-421 which detects local gradients of

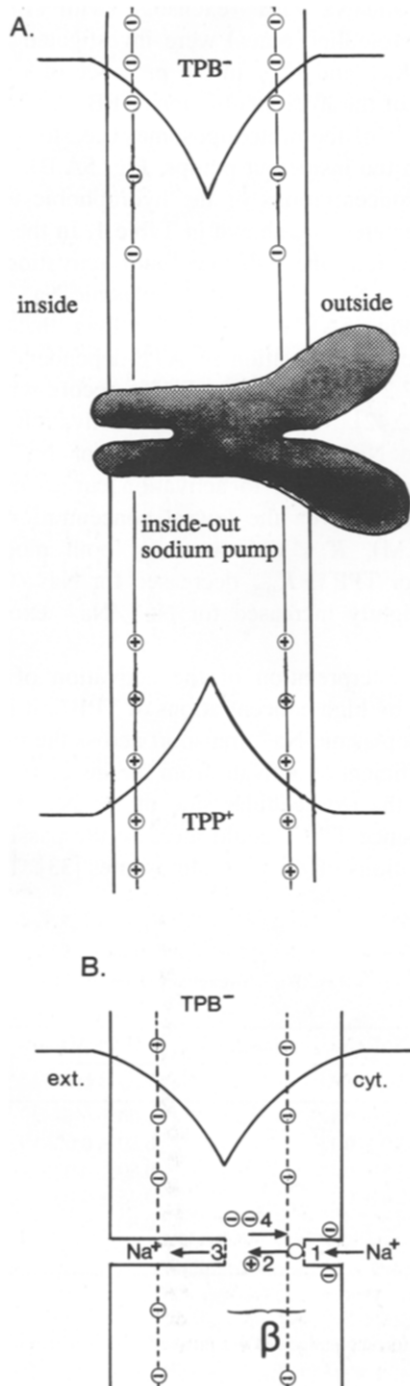


Fig. 3. (A) Electric membrane potential profiles through the lipid bilayer created by either  $\text{TPB}^-$  or  $\text{TPP}^+$  at steady state. The potential profiles in the membrane are drawn assuming rigid lattices of discrete charges from the hydrophobic ions partitioning into the membrane leaving their counterions at the surfaces, and an exponentially decreasing dielectric constant from 80 in the medium to 3 in the centre of the membrane [36]. The potential profiles do not incorporate the dipole potentials [37]. By the addition of the hydrophobic ions to the outside of the proteoliposomes, the electrostatic profile will initially be asymmetric (not shown), reflecting the predominant adsorption of hydrophobic ions near the external water/bilayer interface with the creation of a transmembrane potential which is inside positive in the case of  $\text{TPP}^+$ , and inside negative, in the case of  $\text{TPB}^-$ . Redistribution of the hydrophobic ions within the bilayer establishes a symmetrical potential profile and the transmembrane potential vanishes. Also shown is a schematic drawing of an inside-out inserted sodium-pump protein with a narrow, extracellular ion well and the putative shallow, cytoplasmic ion well indicated. (B) Electrostatic model depicting conceivable voltage-dependent steps during  $\text{Na}^+/\text{O}$  exchange within the sodium pump in the presence of  $\text{TPB}^-$ . Step 1 is the binding of cytoplasmic  $\text{Na}^+$  to 3 sites, two of which are assumed negatively charged within a shallow access channel. Step 2 involves the deocclusion transition. Step 3 is the following release to the extracellular side through a deep ion well, extending half the membrane dielectric distance, which in this simplified model is set equivalent to the physical distance. Step 4 involves the presumed returning of uncompensated negatively charged sites through a certain dielectric distance of the electric field,  $\beta$ .

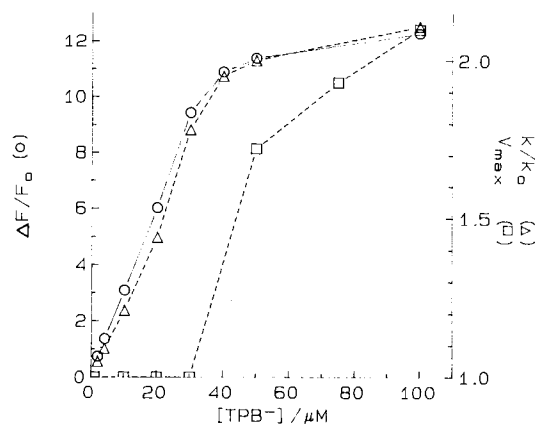


Fig. 4. Fluorescence change ( $\Delta F/F_0$ ) from the electrochromic RH-421 styryl dye incorporated into  $\text{Na}^+, \text{K}^+$ -ATPase proteoliposomes upon addition of hydrophobic ions  $\text{TPB}^-$ . 50  $\mu\text{l}$  proteoliposomes with PC/PE/PI/cholesterol = 48:12:2:38 (mole fractions) prepared to contain 260 mM sucrose, 2 mM  $\text{MgCl}_2$  and 30 mM histidine, pH 7.0 were added to a cuvette containing 2 ml of a buffer solution (NaCl 130 mM,  $\text{MgCl}_2$  2 mM, histidine 30 mM, pH 7.0) and equilibrated with 2  $\mu\text{l}$  RH-421 (1 mg/ml in DMSO).  $\text{TPB}^-$  was then added to give the final concentrations indicated in the figure. The excitation and emission wavelengths were 580 nm and  $> 630$  nm, respectively. As seen the dependence of fluorescence change of RH-421 on  $\text{TPB}^-$  concentration ( $\circ$ ) is approximately linear up to 30  $\mu\text{M}$   $\text{TPB}^-$ , after which the response is progressively suppressed, probably as a consequence of limiting space charge. Essentially identical results were obtained when proteoliposomes prepared without cholesterol were used. For comparison, the calculated relative change of a voltage dependent rate constant ratio  $k/k_0$  is shown by  $\Delta$ . In the latter, it assumes that the membrane potential is proportional to the relative fluorescence increase saturating at a limiting internal membrane potential of  $-100$  mV. The fraction of the effective dielectric that the binding sites move,  $\beta$ , is set to 0.19 (see text for details). The measured activation,  $V_{\text{max}}$  of  $\text{Na}^+/\text{O}$  exchange (indicated by  $\square$ ) is also shown.

electrostatic potentials in the membrane [39].  $\text{TPB}^-$  addition to membrane fragments in concentrations in the micromolar range causes a substantial increase in the fluorescence signal which saturates at  $\text{TPB}^-$  concentrations of 100–150  $\mu\text{M}$  [39]. In the present study the same effects are found using proteoliposomes with reconstituted  $\text{Na}^+, \text{K}^+$ -ATPase (Fig. 4). As indicated, a deflection in the

relative fluorescence starts at about 30  $\mu\text{M}$   $\text{TPB}^-$  and saturation takes place above 100  $\mu\text{M}$ . Identical relative RH-responses,  $\Delta F/F_0$ , (but not their absolute response) were found using proteoliposomes without cholesterol (not shown), indicating that the gradient of electrostatic potential (but not its value) is unchanged by cholesterol as detected by the adsorbed RH fluorochrome.

### 3.4. Cytoplasmic $\text{Na}^+$ activation

The activation curves of cytoplasmic  $\text{Na}^+$  for both  $\text{Na}^+/\text{O}$  (with sucrose and no alkali cations in the proteoliposomes) and  $\text{Na}^+/\text{Na}^+$  exchange (with 117 mM  $\text{Na}^+$  inside the proteoliposomes) were investigated in order to determine  $K_{0.5}$  and  $V_{\text{max}}$  in the presence of varying concentrations of the hydrophobic ions  $\text{TPB}^-$  or  $\text{TPP}^+$  added to the outside of the proteoliposomes (i.e., to the cytoplasmic side on the inside:out pumps, Fig. 5A,B). The effects of varied concentrations of the hydrophobic ions on the kinetic parameters are shown in Table 1. In the absence of hydrophobic ions the half-maximum activation ( $K_{0.5}$ ) of the uncoupled  $\text{Na}^+$  efflux by cytoplasmic  $\text{Na}^+$  was  $5.8 \pm 0.2$  mM (Fig. 5A), a little lower than that found for cytoplasmic  $\text{Na}^+$ -activation of ATP-dependent  $\text{Na}^+/\text{Na}^+$  exchange,  $7.2 \pm 0.1$  mM (Fig. 5B) in accord with previous findings [32,42]. When the control activation curves for cytoplasmic  $\text{Na}^+$  for either  $\text{Na}^+/\text{O}$ , or  $\text{Na}^+/\text{Na}^+$  exchange were compared to activation curves measured in the presence of even the lowest concentration of  $\text{TPB}^-$  used (1  $\mu\text{M}$ ),  $K_{0.5}$  decreased for both modes of exchanges. For  $\text{TPP}^+$ ,  $K_{0.5}$  decreased for  $\text{Na}^+/\text{O}$  exchange but was slightly increased for  $\text{Na}^+/\text{Na}^+$  exchange (see Table 1).

For the interpretation of the activation of uncoupled  $\text{Na}^+$  efflux by high concentrations of  $\text{TPB}^-$ , it is critical to prevent cytoplasmic  $\text{Na}^+$  transport across the bilayer in an amount sufficient to activate from the inside of the proteoliposomes, the extracellular side of the  $\text{Na}^+, \text{K}^+$ -ATPase, especially since  $\text{TPB}^-$  could increase the passive conductance for cations of the proteoliposomes [33]. Therefore, a

Table 1

Dependence on kinetic parameters determined from activation curves of either uncoupled  $\text{Na}^+$  efflux ( $\text{Na}^+/\text{O}$  exchange) or  $\text{Na}^+/\text{Na}^+$  exchange by cytoplasmic  $\text{Na}^+$  on the presence of different hydrophobic ions

	$\text{Na}^+/\text{O}$ exchange ( $\text{Na}_{\text{ext}}^+ = 0$ )		$\text{Na}^+/\text{Na}^+$ exchange ( $\text{Na}_{\text{ext}}^+ = 117$ mM)	
	$K_m$ (mM)	$V_{\text{max}}$ (rel)	$K_m$ (mM)	$V_{\text{max}}$ <sup>a</sup> (rel)
Control	$5.8 \pm 0.2$	1.00 <sup>b</sup>	$7.2 \pm 0.1$	1.00 <sup>b</sup>
$\text{TPB}^-$ (1 $\mu\text{M}$ )	$3.3 \pm 0.2$	$1.02 \pm 0.03$	$5.9 \pm 0.1$	$0.80 \pm 0.02$
$\text{TPB}^-$ (10 $\mu\text{M}$ )	$2.8 \pm 0.2$	$1.14 \pm 0.08$	$3.5 \pm 0.1$	$0.80 \pm 0.02$
$\text{TPB}^-$ (100 $\mu\text{M}$ )	$2.2 \pm 0.1$	$2.10 \pm 0.08$	$2.4 \pm 0.1$	$0.45 \pm 0.06$
$\text{TPP}^+$ (100 $\mu\text{M}$ )	$2.6 \pm 0.4$	$0.56 \pm 0.05$	$9.2 \pm 0.2$	$0.80 \pm 0.10$
$\text{TPP}^+$ (500 $\mu\text{M}$ )	$2.3 \pm 0.2$	$0.46 \pm 0.13$	$9.2 \pm 0.2$	$0.38 \pm 0.10$

The values given are means  $\pm$  S.E. ( $n = 3$ ).

<sup>a</sup> The value depends on the extracellular (intraliposomal)  $\text{Na}^+$  concentration.

<sup>b</sup> The relative values corresponds to maximal hydrolytic activities of  $55 \pm 8$   $\mu\text{mol}/\text{mg}$  per h for uncoupled  $\text{Na}^+$  efflux and  $198 \pm 9$   $\mu\text{mol}/\text{mg}$  per h for  $\text{Na}^+/\text{Na}^+$  exchange, respectively.

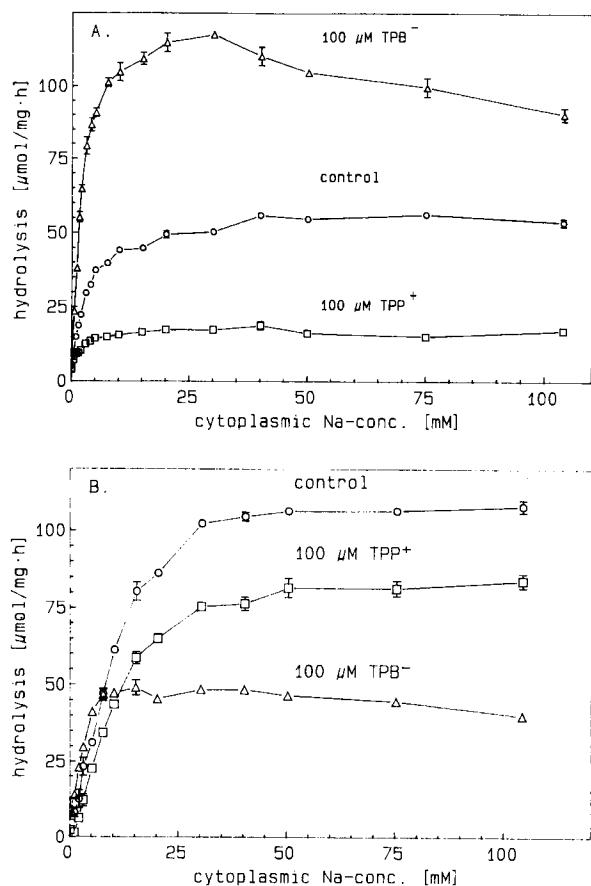


Fig. 5. Effects of TPB<sup>-</sup> (100 μM) and TPP<sup>+</sup> (100 μM) on the rate of ATP-hydrolysis accompanying uncoupled Na<sup>+</sup> efflux (panel A) and Na<sup>+</sup>/Na<sup>+</sup> exchange (panel B) at increasing cytoplasmic Na<sup>+</sup>. Proteoliposomes were prepared in either 130 mM NaCl, 2 mM MgCl<sub>2</sub>, 30 mM histidine (pH 7.0), or with 260 mM sucrose in place of NaCl. The test medium contained: Na<sup>+</sup> at varying concentrations replaced isosmotically with sucrose, ATP 25 μM, Mg<sup>2+</sup> 1 mM, histidine 30 mM and <sup>32</sup>P]ATP at a specific activity of 7.7 · 10<sup>13</sup> cpm/mol. Means ± S.E. (n = 3) are shown.

short assay time and omission of Na<sup>+</sup> during the necessary preincubation with ouabain to inhibit n-o oriented enzyme molecules was found to be important (see Methods).

In proteoliposomes containing ~40 mol% cholesterol  $V_{\max}$  for the uncoupled Na<sup>+</sup>-efflux was unaffected by TPB<sup>-</sup> in concentrations up to 30 μM, after which an increase to more than twice the control value ( $2.13V_{\max} \pm 0.08$ ) was observed when the concentration of TPB<sup>-</sup> was raised to 100 μM or more. In the absence of cholesterol in the liposome bilayer the TPB<sup>-</sup> concentration needed to observe this maximum activation of uncoupled Na<sup>+</sup> efflux was lowered to less than half of that needed in its presence (data not shown).

For Na<sup>+</sup>/Na<sup>+</sup> exchange the  $V_{\max}$  decreased a little for small concentrations of TPB<sup>-</sup>, but was decreased to 50% for 100 μM, and the magnitude of this inhibition depended strongly on the extracellular Na<sup>+</sup> concentration (see below).

As indicated in the activation curves where 100 μM TPB<sup>-</sup> was included, the pronounced activation of uncoupled Na<sup>+</sup> efflux was partially reversed at high cytoplasmic Na<sup>+</sup> concentrations (Fig. 5A), and also for Na<sup>+</sup>/Na<sup>+</sup> exchange a small inhibition was observed at high Na<sup>+</sup><sub>cyt</sub> values (Fig. 5B). This biphasic shape with inhibition at high cytoplasmic [Na<sup>+</sup>] was observed only for the high (100 and 200 μM) TPB<sup>-</sup> concentrations, whereas for lower TPB<sup>-</sup> concentrations it was absent, unless cholesterol was excluded from the bilayer. In this case biphasic activation curves with inhibition at high cytoplasmic [Na<sup>+</sup>] was observed even at 10 μM TPB<sup>-</sup> (not shown).

For TPP<sup>+</sup> a decrease in  $V_{\max}$  to almost half ( $0.56V_{\max} \pm 0.05$ ) was seen in uncoupled Na<sup>+</sup> efflux, whereas turnover was less affected (20–25% decreased) for Na<sup>+</sup>/Na<sup>+</sup> exchange, Fig. 5B. However, if proteoliposomes were used that had not been preincubated with MgP<sub>i</sub> + ouabain, leaving the non-oriented Na<sup>+</sup>,K<sup>+</sup>-ATPase molecules with both sides exposed active, the fractional inhibition by TPP<sup>+</sup> increased (not shown). This apparently assigns the inhibitory effects of TPP<sup>+</sup> predominantly to the extracellular side of the sodium-pump.

### 3.5. Extracellular Na<sup>+</sup>

The effect of the lipophilic ions on the Na<sup>+</sup>/Na<sup>+</sup> exchange was also tested at varying extracellular Na<sup>+</sup> concentrations using proteoliposomes containing different concentrations of Na<sup>+</sup>. Results from such experiments are susceptible to much greater experimental variations since each point in the activation curves represents data from a separate proteoliposome batch. The activities were corrected for differences in reconstituted protein content, whereas the fraction of i:o-orientation was assumed to be independent of [Na<sup>+</sup>]. In Fig. 6A and B the results from a series of experiments are shown in which the intraliposomal Na<sup>+</sup> concentration was varied and the hydrolytic activity tested either near the concentration of cytoplasmic Na<sup>+</sup> (10 mM, Fig. 6A) that gave maximum activation with 100 μM TPB<sup>-</sup>, or at saturating [Na<sup>+</sup>] = 104 mM, (Fig. 6B). In controls, an increasing activity with increasing extracellular [Na<sup>+</sup>] was observed, however, the shape of the curve with intermediate plateau region is too complex to justify an actual determination of a  $K_m$  for extracellular Na<sup>+</sup> (see Cornelius and Skou [42]).

The concentrations of TPB<sup>-</sup> and cytoplasmic Na<sup>+</sup> were critical for the observed effects of extracellular Na<sup>+</sup> activation: at 1 μM TPB<sup>-</sup>, the hydrolysis for all extracellular [Na<sup>+</sup>] tested was similar to controls, at both 10 mM and 104 mM cytoplasmic Na<sup>+</sup> (not shown). For 100 μM TPB<sup>-</sup> and 10 mM cytoplasmic Na<sup>+</sup>, hydrolysis was increased at all extracellular [Na<sup>+</sup>], except for the highest concentration (Fig. 6A). At 104 mM cytoplasmic Na<sup>+</sup>, TPB<sup>-</sup> also activated at low extracellular [Na<sup>+</sup>], but inhibition was observed already at extracellular Na<sup>+</sup>-concentrations above 25 mM.

Temperature is also critical for these effects of  $\text{TPB}^-$ : At decreasing temperature the activation at small extracellular  $[\text{Na}^+]$  (including  $[\text{Na}^+] = 0$  mM) increases and the partial inhibition observed at high extracellular  $\text{Na}^+$  vanishes (Fig. 7). At  $0^\circ\text{C}$   $100\ \mu\text{M}$   $\text{TPB}^-$  increases hydrolysis accompanying uncoupled  $\text{Na}^+$ -efflux by 400% (Fig. 7).

$\text{TPP}^+$  decreased the hydrolytic capacity for all extracellular  $\text{Na}^+$  concentrations, including  $[\text{Na}^+]_{\text{ext}} = 0$  mM (uncoupled efflux), at both 10 mM cytoplasmic  $\text{Na}^+$  and at 104 mM cytoplasmic  $\text{Na}^+$  (Fig. 6A, B).

### 3.6. Surface charge and dipole potential from lipid composition

The phospholipid composition of the proteoliposomes, e.g., the presence of charged phospholipids like phosphatidyl inositol (PI), can have substantial effects on the surface charge of the bilayer. However, proteoliposomes prepared to contain only phosphatidylcholine (PC) and cholesterol (chol) (PC/chol = 62:38 mol fraction) gave essentially the same results as the standard proteoliposomes which contained also PI and phosphatidyl-

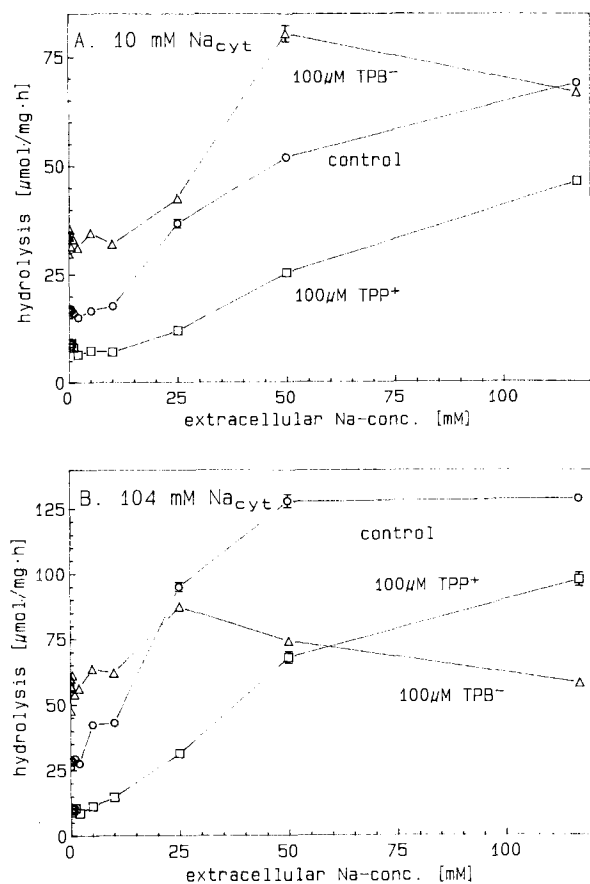


Fig. 6. Effects of hydrophobic ions on extracellular  $\text{Na}^+$  activation at two different cytoplasmic  $\text{Na}^+$  concentrations. Panel A depicts activation curves at  $20^\circ\text{C}$  in the presence of  $100\ \mu\text{M}$   $\text{TPB}^-$ , and  $100\ \mu\text{M}$   $\text{TPP}^+$  compared to control values at 10 mM cytoplasmic  $\text{Na}^+$ . Panel B shows the effects of hydrophobic ions at 104 mM cytoplasmic  $\text{Na}^+$ . Data points represent means  $\pm$  S.E. ( $n = 3$ ).

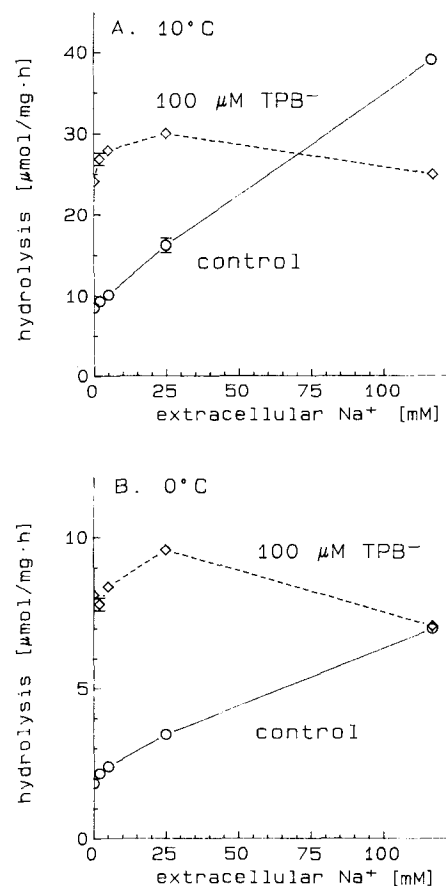


Fig. 7. Temperature dependence of  $\text{TPB}^-$  effects on extracellular  $\text{Na}^+$  activation. Activation curves determined at 104 mM cytoplasmic  $\text{Na}^+$  at  $10^\circ\text{C}$  (A) and at  $0^\circ\text{C}$  (B) are shown. Compare with Fig. 6B at  $20^\circ\text{C}$ .

ethanolamine (PE) (PC/PE/PI/chol = 48:12:2:38 mol fractions) with respect to their effects on both catalysis and dephosphorylation rate. This is consistent with the notion that the dominating factor for the surface dipole potential is the cholesterol content [43,44] which was constant in the different proteoliposome preparations.

### 3.7. Phosphorylation / dephosphorylation

In both  $\text{Na}^+/\text{Na}^+$  and  $\text{Na}^+/0$  exchange the dephosphorylation step is considered rate determining [46]. Accordingly, it was investigated if the rate of spontaneous dephosphorylation was affected by the hydrophobic cation and anion under conditions of either uncoupled  $\text{Na}^+$  efflux or  $\text{Na}^+/\text{Na}^+$  exchange and compared to the maximum rate of hydrolysis. A lower temperature of  $10^\circ\text{C}$  was used for accurate determination of dephosphorylation rate. For uncoupled  $\text{Na}^+$  efflux the maximum hydrolytic activity at  $10^\circ\text{C}$  was found to be  $10.8 \pm 0.5\ \mu\text{mol}/\text{mg}$  per h (mean  $\pm$  S.D.,  $n = 3$ ) compared to  $30.5 \pm 0.2\ \mu\text{mol}/\text{mg}$  per h (mean  $\pm$  S.D.,  $n = 6$ ) for  $\text{Na}^+/\text{Na}^+$  exchange, i.e., an approx. 6-fold reduction for both by decreasing the temperature from  $20^\circ\text{C}$  to  $10^\circ\text{C}$ .



Table 2

Dependence of hydrophobic ions on rate constants ( $s^{-1}$ ) for the dephosphorylation reaction at  $10^{\circ}C$  in the absence of extracellular  $Na^{+}$  ( $Na^{+}/0$ ) and in its presence ( $Na^{+}/Na^{+}$ )

	$Na^{+}/0$ ( $Na_{ext} = 0$ mM)		$Na^{+}/Na^{+}$ ( $Na_{ext} = 117$ mM)	
	$\tau_1$	$\tau_2$	$\tau_1$	$\tau_2$
Control	$0.074 \pm 0.001$	—	$0.055 \pm 0.018$ (39 $\pm$ 4.9)	$0.528 \pm 0.034$ (61 $\pm$ 4.9)
TPB $^{-}$ (1 $\mu$ M)	$0.079 \pm 0.003$	—	$0.036 \pm 0.004$ (41 $\pm$ 4.7)	$0.389 \pm 0.027$ (59 $\pm$ 5.9)
TPB $^{-}$ (100 $\mu$ M)	$0.159 \pm 0.016$	—	$0.038 \pm 0.011$ (21 $\pm$ 5.8)	$0.482 \pm 0.071$ (79 $\pm$ 5.8)
TPP $^{+}$ (100 $\mu$ M)	$0.051 \pm 0.001$	—	$0.039 \pm 0.004$ (40 $\pm$ 2.5)	$0.439 \pm 0.079$ (60 $\pm$ 2.5)

Values are means  $\pm$  S.D. ( $n = 3$  for  $Na^{+}/0$  and  $n = 4$  for  $Na^{+}/Na^{+}$ ). Numbers in parenthesis are fractions in % of the EP-pool, which dephosphorylated with indicated time constant. The coefficient of correlation ( $r$ ) is for all fits better than 0.997. No parameters were fixed in the fitting procedure.

Below 100  $\mu$ M TPB $^{-}$  had no effect on dephosphorylation rate of neither uncoupled efflux nor  $Na^{+}/Na^{+}$  exchange. However, at 100  $\mu$ M TPB $^{-}$  increased the rate of spontaneous dephosphorylation in the absence of extracellular  $Na^{+}$  (Fig. 8A), but left it largely unaffected in the presence of 117 mM  $Na^{+}$  inside the proteoliposomes (Fig. 8B). TPP $^{+}$  decreased the rate of dephosphorylation in  $Na^{+}/0$  exchange, and the rate of dephosphorylation slightly in  $Na^{+}/Na^{+}$  exchange with 117 mM internal  $Na^{+}$ . Therefore, parallel effects of TPB $^{-}$ /TPP $^{+}$  on the rate of dephosphorylation and turnover of hydrolysis were found for  $Na^{+}/0$ . For  $Na^{+}/Na^{+}$  exchange TPB $^{-}$  and TPP $^{+}$  acted with less effect on the rate of dephosphorylation than on the turnover of hydrolysis, indicating that their effects were mainly on other reactions.

In Table 2 the parameters for a computer analysis where the dephosphorylation curves were fitted to exponentials are given. As indicated, in the absence of extracellular  $Na^{+}$  monoexponential and biexponential curves fit the data equally well with rate constants that depended on which hydrophobic ions were present. In the presence of 117 mM extracellular  $Na^{+}$  the dephosphorylation curves were clearly biexponential with a substantial component

disappearing with a much faster decay rate than in the absence of extracellular  $Na^{+}$ .

In all conditions studied the hydrophobic ions were without significant effect on either the rate of phosphoryla-

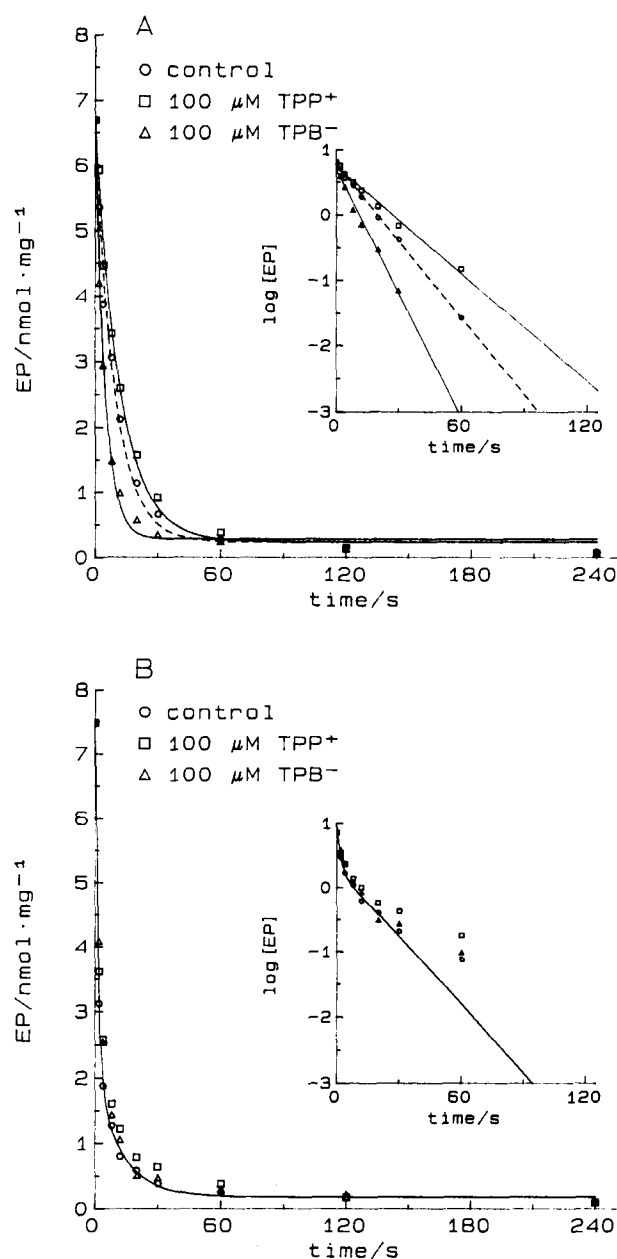


Fig. 8. TPB $^{-}$  and TPP $^{+}$  effects on dephosphorylation of phosphoenzyme at  $10^{\circ}C$  using reconstituted inside-out  $Na^{+},K^{+}$ -ATPase in the absence of extracellular  $Na^{+}$  (panel A) and in the presence of 114 mM extracellular  $Na^{+}$  (panel B). In both cases the concentration of  $Na^{+}$  in the medium (cytoplasmic) is 65 mM. The curves are best fit to a monoexponential function of the form:  $Y = A \cdot \exp(-BX) + E$  (panel A) or to a biexponential equation of the form:  $Y = A \cdot \exp(-BX) + C \cdot \exp(-DX) + E$  (panel B). The fitted rate coefficient for uncoupled  $Na^{+}$  efflux (panel A) is:  $0.104 \pm 0.009$   $s^{-1}$ ,  $0.212 \pm 0.013$   $s^{-1}$ , and  $0.083 \pm 0.006$   $s^{-1}$  for control, TPB $^{-}$ , and TPP $^{+}$ , respectively. The residuals were  $0.24 \pm 0.1$  (parameter  $E$  in exponential equation above). The corresponding fitted steady-state EP levels are:  $6.3 \pm 0.2$  nmol/mg,  $6.3 \pm 0.2$  nmol/mg, and  $6.4 \pm 0.2$  nmol/mg. For  $Na^{+}/Na^{+}$  exchange monoexponential equations did not fit the data as judged by  $F$ -tests and at least biexponential equations had to be used. The three fitted decay curves (control, +TPB $^{-}$ , and +TPP $^{+}$ ) differ insignificantly and therefore only the fit to the control-curve is shown. The fitted values correspond to rate coefficients of  $0.080 \pm 0.014$   $s^{-1}$  (EP fraction  $1.91 \pm 0.26$  nmol/mg) and  $0.704 \pm 0.062$   $s^{-1}$  (EP fraction  $5.39 \pm 0.27$  nmol/mg), with a residual of  $0.2 \pm 0.05$ . The insets show logarithmic transforms of the data (corrected for residuals) and curve fit.

tion (not shown) or the steady-state level of phosphorylation. In reconstituted  $\text{Na}^+, \text{K}^+$ -ATPase the number of phosphorylation sites was consistently found to be  $7.1 \pm 0.5$  nmol/mg i:o oriented protein (mean  $\pm$  S.D.,  $n = 5$ ), corresponding to one phosphorylation site per  $\alpha\beta$  protomer [45].

#### 4. Discussion

There is compelling evidence that the electrogenicity of the sodium-limb in the  $\text{Na}^+, \text{K}^+$ -ATPase reaction cycle (Fig. 1) can be accounted for by the release of  $\text{Na}^+$  through an extracellular narrow access channel [14,16–19,21,47,48]. In contrast, the pathway which during physiological conditions translocates extracellular  $\text{K}^+$  (the 'potassium-limb') was generally thought to be electroneutral [11,12,16,25,49–51], but during conditions of low extracellular  $\text{K}^+$  a voltage dependency can be shown [22,52,53]. The observations seem to provide strong evidence against conformational changes occurring in the  $\text{K}^+$ -limb to be electrogenic themselves, whereas the binding of extracellular  $\text{K}^+$  could still be voltage dependent. However, if the two putative compensating negative charges in the binding domain for cytoplasmic  $\text{Na}^+$  'return' uncompensated in the uncoupled  $\text{Na}^+$  efflux mode, this limb switches from electroneutral in the presence of extracellular alkali cations to electrogenic in their absence. It may therefore be possible to detect if steps along this pathway in uncoupled mode involve displacements of charged binding sites through the membrane dielectric by imposing inner membrane potentials which could affect the turnover rate, since it is steps along this pathway that are believed to be rate-determining in the absence of extracellular  $\text{K}^+$  [46].

In the present study the hydrophobic ions  $\text{TPB}^-$  and  $\text{TPP}^+$  were indeed found to affect both the turnover rate and the cation affinity, depending on which partial reaction of the  $\text{Na}^+, \text{K}^+$ -ATPase was studied. These effects may be explained from electrostatic interactions induced by the hydrophobic ions, which adsorb strongly to lipid bilayers, creating internal electrostatic potentials also extending to the incorporated  $\text{Na}^+, \text{K}^+$ -ATPase, which has a dielectric constant between 3 and 4, comparable to that of the pure bilayer [37,54].

The shape of the imposed electrostatic potential gradient will depend both on the location of the adsorption plane for the hydrophobic ions and on the dielectric nature of the bilayer and the protein. The adsorption plane for  $\text{TPP}^+/\text{TPB}^-$  is probably located about 2 nm within each water/lipid interface [38,55], however others place them further out [35,56], depending also on the ionic strength of the medium. Unfortunately, the partition coefficients for the two otherwise structurally very similar hydrophobic ions  $\text{TPB}^-$  and  $\text{TPP}^+$  differ by at least three orders of magnitude, which could indicate huge differences in their

free concentrations in order to compare their electrostatic effects. The reason for this, the inner positive membrane dipole potential, further complicates the situation. Apart from the electrostatic interactions of the hydrophobic ions on the  $\text{Na}^+, \text{K}^+$ -ATPase, direct chemical effects, e.g., by binding to hydrophobic domains, as well as changes in bilayer fluidity or dielectric constant, also have to be considered.

##### 4.1. Effects of hydrophobic ions on turnover and dephosphorylation

The observed effects of the hydrophobic ions on the half-maximum activation for hydrolysis of cytoplasmic  $\text{Na}^+$ ,  $K_{0.5}$ , and on the maximum hydrolytic activity,  $V_{\max}$ , are complicated to interpret, especially since such steady-state kinetic parameters may depend on several rate constants and ligand concentrations. However, if the effects of the hydrophobic ions on turnover rate are caused by their electrostatic interaction with putative electrogenic pathways in the pumping action, which could it then be? The situation could be illustrated as depicted in Fig. 3B, assuming a shallow cytoplasmic and a deep extracellular access channel. In such a simplified model the voltage-dependency of  $\text{Na}^+/\text{O}$  exchange could in principle arise from electrostatic interaction with either one of the following reactions: (1) Cytoplasmic  $\text{Na}^+$ -binding, if any one of the three cytoplasmic  $\text{Na}^+$  has to approach their binding sites through a high-field access channel [21,25]. (2) The phosphorylation step or the deocclusion of  $\text{E}_1\text{P}(\text{Na})_3 \rightarrow \text{E}_1\text{PNa}_3$ , if these transitions are associated with charge movement [12]. (3) The release of  $\text{Na}^+$  to the extracellular side through a deep high-field access channel, spanning about half the effective membrane dielectric [18]. (4) The dephosphorylation and/or deocclusion of 'empty'  $\text{E}_2\text{O}$ , if this transition involves the returning of uncompensated, negative binding sites [12,25]. If the effects of the hydrophobic ions  $\text{TPB}^-/\text{TPP}^+$  on  $V_{\max}$  in  $\text{Na}^+/\text{O}$  exchange is first considered using this simple 4-step model, which of these steps could then be involved?

The phosphorylation reaction itself (step 2) has been shown not to be a charge carrying step [14], in agreement with our own observations that neither  $\text{TPB}^-$  nor  $\text{TPP}^+$  have any significant effects on the kinetics of phosphorylation reactions during both  $\text{Na}^+/\text{O}$  exchange and  $\text{Na}^+/\text{Na}^+$  exchange (data not shown). Recent observations have indicated that the conformational change associated with the deocclusion of  $\text{Na}^+$  is in itself also electroneutral, since the voltage-dependency of  $\text{Na}^+$  release is apparently restricted to electrostatic interaction with the  $\text{Na}^+$  binding rate coefficient [17,18]. At any rate, this reaction (step 3) will be decelerated by the negative membrane potential induced by  $\text{TPB}^-$ , and accelerated by  $\text{TPP}^+$ , given the indicated localization of the extracellular ion well (Fig. 3B), giving the opposite effect of the observed. Step 1 would in theory be affected by  $\text{TPB}^-/\text{TPP}^+$  changing the

binding affinity for cytoplasmic  $\text{Na}^+$ , as will be considered in the end of the discussion, but without enhancing in itself the maximum turnover rate ( $V_{\text{max}}$ ), since this step is not supposed to be rate determining. This leaves step 4, the dephosphorylation, as the most likely site for electrostatic interaction. With the indicated localization of the extracellular deep access channel these steps proceed within the inner half of the membrane dielectric and would be accelerated by an inner negative potentials ( $\text{TPB}^-$ ) and decelerated by an inner positive potentials ( $\text{TPP}^+$ ), affecting  $V_{\text{max}}$  in the expected directions.

It could be argued that the effect of  $\text{TPB}^-$  was to make the proteoliposomes leaky to  $\text{Na}^+$ , thereby activating turnover by switching from uncoupled  $\text{Na}^+$  efflux to the  $\text{Na}^+/\text{Na}^+$  exchange mode. However, this is not in accord with the fact that activation is observed at low concentrations of  $\text{Na}^+_{\text{cyt}}$  and not at higher concentrations, and that  $\text{TPB}^-$  activates the hydrolysis to levels above that found in proteoliposomes produced with optimum internal  $\text{Na}^+$  and in the absence of  $\text{TPB}^-$ , at least at temperatures below  $20^\circ\text{C}$ .

The high concentrations of  $\text{TPB}^-$  needed to induce an acceleration of uncoupled  $\text{Na}^+$ -efflux could be taken to indicate effects from either direct chemical interaction with the  $\text{Na}^+,\text{K}^+$ -ATPase, e.g., to hydrophobic membrane segments, or from changes in membrane fluidity and dielectric constant. Such possibilities are difficult to exclude, however Klodos and Plesner [57] did not find indications on direct interactions at high  $[\text{TPB}^-] = 33\ \mu\text{M}$  using unsided membrane preparations, and to explain the present results very complicated interactions with the  $\text{Na}^+$ -concentrations in the medium on such putative  $\text{TPB}^-$ -binding to the enzyme would have to be assumed. A more likely explanation is that the effect of  $\text{TPB}^-$  is impeded by the inside positive dipole potential of cholesterol. Such interferences with the electrostatic potential profile of the hydrophobic ions are clearly demonstrated in experiments by Franklin and Cafiso [44] showing that 6-ketocholestanol affects both the binding and translocation rate constant of hydrophobic ions. In addition the high concentration of  $\text{TPB}^-$  could also be required in order to push the adsorption plane of the hydrophobic ion further outward towards the phospholipid headgroups for maximal interaction with electrogenic steps in the proposed pathway in the uncoupled  $\text{Na}^+$  reaction to take place. Ellena et al. [55] find such shifts in adsorption plane for  $\text{TPB}^-$  at concentrations above 10 mol%  $\text{TPB}^-$ .

How does the proposed explanation compare with the observed effects of  $\text{TPB}^-/\text{TPP}^+$  on  $V_{\text{max}}$  in  $\text{Na}^+/\text{Na}^+$  exchange?  $\text{TPP}^+$  decreases the turnover rate at all extracellular  $\text{Na}^+$  concentrations (Fig. 6A,B). An inside positive electrostatic potential should accelerate  $\text{Na}^+$  release and oppose  $\text{Na}^+$  binding at the extracellular side, if extracellular  $\text{Na}^+$  has to pass a narrow access channel (ion well) to depart from or arrive at its extracellular binding sites in the protein interior. Since inhibition of hydrolysis is observed,

$\text{TPP}^+$  inhibition of the  $\text{Na}^+$  binding process is apparently predominant, as also previously suggested [20,21], with a resulting decreased rate of turnover.

In contrast, the effects of  $\text{TPB}^-$  on extracellular  $\text{Na}^+$  activation are critically dependent on the concentration of cytoplasmic  $\text{Na}^+$ : at 10 mM, activation of turnover is observed for all extracellular  $\text{Na}^+$  concentrations except the highest (117 mM, Fig. 6A). This can be explained along the same lines as for  $\text{TPP}^+$ , namely, that the established internal electrostatic potential (here negative) enhances the binding of extracellular  $\text{Na}^+$  by modifying the electrostatic energy, or raising the effective  $\text{Na}^+$ -concentration at binding sites located in an ion-well. At low cytoplasmic  $\text{Na}^+$ , the enhanced binding affinity for extracellular  $\text{Na}^+$  apparently overcomes the depressing effect of  $\text{TPB}^-$  on  $\text{Na}^+$  release, and activation results. However, at high concentrations of cytoplasmic  $\text{Na}^+$  (104 mM), extracellular  $\text{Na}^+$  in concentrations above 25 mM inhibits turnover (Fig. 6B). This indicates that now the release of extracellular  $\text{Na}^+$  through the ion-well also becomes limiting. This could also explain the decrease in activation at increasing cytoplasmic  $\text{Na}^+$  in uncoupled  $\text{Na}^+$ -efflux (Fig. 5A).

The effects of hydrophobic ions on uncoupled  $\text{Na}^+$ -efflux and  $\text{Na}^+/\text{Na}^+$  exchange can therefore in principle be interpreted from electrostatic interactions at the extracellularly located ion well together with effects on some steps along the pathway translocating empty, negatively charged sites in the uncoupled  $\text{Na}^+$ -efflux mode. The latter is consistent with the simple electrostatic model [12,25] in which two negatively charged groups accompany the translocation of three cytoplasmic  $\text{Na}^+$  to the extracellular side and return to the cytoplasmic side either uncompensated, as in uncoupled  $\text{Na}^+$  efflux, or neutralized by two extracellular  $\text{Na}^+$ , as in  $\text{Na}^+/\text{Na}^+$  exchange. It is also consistent with the measured net charge stoichiometries of 1 per ATP split in  $\text{Na}^+/\text{Na}^+$  exchange (+1 in the  $\text{Na}^+$ -limb and 0 in the  $\text{K}^+$ -limb) and 3 per ATP split in  $\text{Na}^+/0$  exchange (+1 in the  $\text{Na}^+$ -limb and -2 in the opposite direction in the  $\text{K}^+$ -limb).

If this interpretation is correct, then which of the steps in the return from the extracellular side during  $\text{Na}^+/0$  exchange are to be considered as the major charge translocating ones? The reactions along the pathway that returns the empty sites can be assumed to contain in analogy to the potassium limb two steps as a minimum: a dephosphorylation and an occlusion step  $\text{E}_2\text{P} \rightarrow \text{E}_2\text{O}$ , and a step with deocclusion of 'empty'  $\text{E}_2\text{O}$  by ATP binding,  $\text{E}_2\text{O} + \text{ATP} \rightarrow \text{E}_1\text{ATP}$  (Fig. 1). As seen from Table 2 there is a pronounced effect of the hydrophobic ions on the rate constant for the monoexponential dephosphorylation during uncoupled  $\text{Na}^+$  efflux, indicating that it may be during this reaction that negative charge is moved.

If the forward rate constant in this reaction is denoted  $k$ , then its dependence on electrical potential ( $V$ ) can be described by:  $k = k_0 \cdot \exp(z_L \cdot \beta \cdot V/2)$  [49,58,59], where

$k_0$  is the rate constant in the absence of a potential,  $\beta$  the fraction of the effective dielectric the binding sites moves,  $z_L$  is the charge of the binding sites ( $-2$ ), and  $V$  the potential multiplied with  $(F/RT)$ , the Faraday constant over the gas constant and temperature. With two  $\text{Na}^+$  ions bound the equivalent expression is obtained by exchanging  $z_L$  with  $(2 + z_L)$ . It is clear from this equation that (i) if  $\beta$  is small, i.e., if the binding sites only traverse a small part of the effective membrane dielectric, a considerable membrane potential may have to be applied to see an effect (this could also add to explain the necessity of using high concentrations of  $\text{TPB}^-$  to see effects), and (ii) with extracellular  $\text{Na}^+$  bound the 'potassium-limb' shifts from electrogenic to electroneutral. If the model analysis of Mauzerall and Drain [38] is used to estimate the maximum inner electrostatic potential resulting from lattices of  $100 \mu\text{M}$   $\text{TPB}^-$ , where a charge density of  $\sim 0.2 \text{ nm}^{-2}$  is measured, between  $-70 \text{ mV}$  and  $-140 \text{ mV}$  is calculated in the bilayer centre, depending on whether or not the model used incorporates a constant dielectric of the membrane core. If this potential gradient is fully effective and it is assumed that the doubling in  $V_{\text{max}}$  in uncoupled  $\text{Na}^+$  efflux produced by  $100 \mu\text{M}$   $\text{TPB}^-$  is accounted for entirely by an increase in the dephosphorylation rate constant  $k$  (this disregards any inhibitory effects on  $\text{Na}^+$  release through the extracellular ion well at the concentration of cytoplasmic  $\text{Na}^+$  giving  $V_{\text{max}}$  which is about  $25 \text{ mM}$  in Fig. 5A, see below), an estimation of  $\beta$  gives between  $0.13$  and  $0.25$ . Given the uncertainties in the assumptions made, this means that two negatively charged binding sites have to pass between  $13\%$ – $25\%$  of the total membrane electric field, to account for the experimental results.

The relation between electrostatic potential and rate constant given above can be used to calculate the expected change in enzyme turnover for different concentrations of  $\text{TPB}^-$  given the same assumptions as stated above and that the RH-fluorescence is proportional to the local gradient of electrostatic potential. The calculated results are given in Fig. 4 and compared with the measured values. As indicated, the calculated relative increase in the ratio of rate constant ( $k/k_0$ ) follows the relative increase in RH-fluorescence as a function of  $\text{TPB}^-$  concentration, whereas the measured increase in hydrolysis is lacking behind, indicating that at low  $\text{TPB}^-$  concentrations an inhibition that chancels out the later activation is unaccounted for in the assumptions. This could indicate that the assumption which disregards the retarding effect of  $\text{TPB}^-$  on  $\text{Na}^+$  release through the extracellular ion-well is not fully justified, or it could be due to the earlier mentioned inner positive dipole potential of cholesterol which lowers the inner negative potential induced by  $[\text{TPB}^-]$ . The essential identical relative RH-responses to  $\text{TPB}^-$  in the presence and absence of cholesterol indicate that the inner potential of  $\text{TPB}^-$  is lowered by an equal amount through most of the bilayer leaving the local gradient of potential unchanged at the site where RH is adsorbed.

The  $\text{TPB}^-$  activation of turnover rate during uncoupled  $\text{Na}^+$  efflux can be quantitatively accounted for by its acceleration of the dephosphorylation reaction. As seen from Table 2, the dephosphorylation reaction is biexponential in the presence of extracellular  $\text{Na}^+$ . No straightforward explanation for biphasic dephosphorylation can be given at present. It can be taken to indicate enzyme heterogeneity [60–62] inferring that in pure  $\text{Na}^+$ , at least two phosphoforms are dephosphorylated in parallel. In such a system, the fraction with the faster rate of dephosphorylation, which appears in the presence of extracellular  $\text{Na}^+$ , could conceivably represent dephosphorylation of  $\text{E}_2\text{PNa}_2$  since it is not significantly affected by the charge from the hydrophobic ions (see Table 2). Accordingly, the smaller EP-fraction with a ten-fold lower dephosphorylation rate could represent dephosphorylation of  $\text{E}_2\text{P}$  with no (or one)  $\text{Na}^+$  bound. If this was to be true the two phosphoforms cannot be in rapid equilibrium, in contrast to previous suggestions (see, e.g., Cornelius [63]), since monoexponential dephosphorylation would then result.

The hydrolytic activity measured under identical conditions as for measurements of dephosphorylation (which is non-optimal) correlates with calculated turnover for both  $\text{Na}^+/0$  and  $\text{Na}^+/\text{Na}^+$  exchange if parallel dephosphorylation is assumed, given by the sum of products of rate coefficient and amount of steady-state phosphoenzymes (EP). As seen from Table 2 the proportion of calculated turnover for  $\text{Na}^+/0$  exchange ( $\tau \times \text{EP}$ ) relative to  $\text{Na}^+/\text{Na}^+$  exchange assuming parallel dephosphorylation ( $[\tau_1 \times \text{fraction}_1] + [\tau_2 \times \text{fraction}_2] \times \text{EP}$ ) is  $1:4.5$  which is about the same proportion found if maximum hydrolytic activity is measured for the two modes of exchange ( $55.6 \mu\text{mol/mg per h}$  and  $197.3 \mu\text{mol/mg per h}$ , respectively, giving a ratio of  $1:3.5$ ).

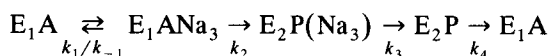
The explanation that the dephosphorylation in the absence of extracellular alkali cations is electrogenic is also in accord with the observation that as the extracellular concentration of  $\text{Na}^+$  increases, the exchange reaction shifts towards  $\text{Na}^+/\text{Na}^+$  exchange with the neutralization of the negatively charged binding sites, and the dissipation of both the accelerating effect of  $\text{TPB}^-$ , as well as the decelerating effect of  $\text{TPP}^+$ .

#### 4.2. Effects of hydrophobic ions on cytoplasmic $\text{Na}^+$ binding

The partition of the hydrophobic ions into the proteoliposome bilayer and the resulting electrostatic potentials inside the bilayer may affect not only the rate of ion-translocation across the bilayer, but also the association/dissociation processes of the ligands ( $\text{Na}^+$ ) to their binding sites on the embedded  $\text{Na}^+/\text{K}^+$ -ATPase [20,21], e.g., if  $\text{Na}^+$  has to pass an ion well to arrive at its binding site.

In both  $\text{Na}^+/0$  exchange and  $\text{Na}^+/\text{Na}^+$  exchange a decrease in apparent  $K_m$  for cytoplasmic  $\text{Na}^+$  is found in the presence of  $\text{TPB}^-$  at concentrations ( $1 \mu\text{M}$  and  $10$

$\mu\text{M}$ ) where  $V_{\max}$  is essentially unchanged (Table 1, Fig. 5A,B). This indicates that  $\text{TPB}^-$  interacts with intermediates with which cytoplasmic  $\text{Na}^+$  is involved. Such interactions could be effects of the inner membrane potential from  $\text{TPB}^-$  on the electrostatic energy of  $\text{Na}^+$  at its cytoplasmic binding sites, as proposed previously to be the case for binding of one of the three cytoplasmic  $\text{Na}^+$  which may migrate to a buried neutral binding site [21,25]. By analogy,  $\text{TPP}^+$  would be expected to decrease the affinity for cytoplasmic  $\text{Na}^+$ . This is in accord with results during  $\text{Na}^+/\text{Na}^+$  exchange (Table 1) where  $K_m$  increases at  $\text{TPB}^-$  concentrations where  $V_{\max}$  is unchanged. However, during  $\text{Na}^+/\text{O}$  exchange both  $V_{\max}$  and the apparent  $K_m$  decrease in proportion making it uncertain to deduce effects by  $\text{TPP}^+$  on the binding affinity of cytoplasmic  $\text{Na}^+$  itself. Since  $K_m$  depends on all the rate constants in the assumed mechanism  $\text{TPP}^+$  interaction with any one of the intermediates will have an effect on  $K_m$ . However, the ratio  $K_m/V_{\max}$  will be dependent only on rate constants characterizing the intermediates with which cytoplasmic  $\text{Na}^+$  is involved [67]. Using the simple 4-step model, mentioned in the beginning of the discussion, in which only four essential steps for the  $\text{Na}^+/\text{O}$  exchange are assumed:



$k$  indicates rate constants in the following reactions: (1) binding and release of cytoplasmic  $\text{Na}^+$ , (2) phosphorylation and occlusion, (3) deocclusion and release of  $\text{Na}^+$  through the extracellular ion-well, and (4) dephosphorylation. The ratio  $K_m/V_{\max}$  depends on the rate constants  $k_{-1}$ ,  $k_1$ ,  $k_2$ , and  $k_3$ . Therefore, the  $\text{TPP}^+$  interaction with the affinity of cytoplasmic  $\text{Na}^+$  (through  $k_{-1}$  and  $k_1$ ) together with an effect on  $k_3$ , the release through the extracellular ion-well, could produce the obtained result that  $K_m$  decreases whereas the ratio  $K_m/V_{\max}$  is only slightly changed. Therefore, an acceleration of  $\text{Na}^+$  release through the extracellular ion-well by an inner positive potential induced by  $\text{TPP}^+$  may mask the decreased cytoplasmic  $\text{Na}^+$  affinity. In the presence of  $\text{TPB}^-$ , where the cytoplasmic  $\text{Na}^+$ -affinity is increased and the  $\text{Na}^+$  release through the extracellular ion-well is decreased, the decrease in apparent  $K_m$  may be potentiated. The same effects could conceivably be produced by effects of  $\text{TPB}^-/\text{TPP}^+$  on  $k_2$ , the phosphorylation. However, this reaction is apparently electroneutral [14].

To summarize, the very complicated effects of  $\text{TPB}^-$  and  $\text{TPP}^+$  on uncoupled  $\text{Na}^+$ -efflux is consistent with their electrostatic interactions at mainly three steps in the reaction sequence: at extracellular and cytoplasmic ion-wells and on a charge translocating step, which is probably the dephosphorylation of 'empty'  $\text{E}_2\text{P}$ . These results are consistent with (but do not prove) the simple electrostatic model in which two negative charges are present in the cytoplasmic  $\text{Na}^+$ -binding domain of the  $\text{Na}^+,\text{K}^+$ -ATPase

and co-migrate during enzyme turn-over [12,25]. During  $\text{Na}^+/\text{Na}^+$  exchange in which extracellular  $\text{Na}^+$  acts as a  $\text{K}^+$  congener the latter reaction becomes electroneutral by extracellular  $\text{Na}^+$ -binding. A parallel charge-translocating step through the membrane dielectric field in the sodium-limb of the  $\text{Na}^+,\text{K}^+$ -ATPase reaction associated with a conformational step is apparently absent since the voltage dependency of the sodium-limb is entirely accounted for by the rebinding of  $\text{Na}^+$  in a high-field extracellular channel [17,18].

## Acknowledgements

I thank Drs. J.C. Skou, R.L. Post, and I. Klodos for useful discussions and Hanne Zakarias for the excellent technical assistance. The financial support of The Danish Medical Research Council, Novo Foundation, Aarhus University Research Foundation, and The Danish Biotechnology Centre for Biomembranes is gratefully acknowledged.

## References

- [1] Garrahan, P.J. and Glynn, I.M. (1967) *J. Physiol.* 192, 159–174.
- [2] Garrahan, P.J. and Glynn, I.M. (1967) *J. Physiol.* 192, 175–188.
- [3] Cornelius, F. (1991) *Biochim. Biophys. Acta* 1071, 19–66.
- [4] Lee, K.H. and Blostein, R. (1980) *Nature* 285, 338–339.
- [5] Blostein, R. (1983) *J. Biol. Chem.* 258, 7948–7953.
- [6] Cornelius, F. and Skou, J.C. (1985) *Biochim. Biophys. Acta* 818, 211–221.
- [7] Cornelius, F. (1989) *Biochem. Biophys. Res. Commun.* 160, 801–807.
- [8] Apell, H.-J., Häring, V. and Roudna, M. (1990) *Biochim. Biophys. Acta* 1023, 8190.
- [9] Fahn, S., Koval, G.J. and Albers, R.W. (1966) *J. Biol. Chem.* 241, 1882–1889.
- [10] Post, R.L., Kume, S., Tobin, T., Orcutt, B. and Sen, A.K. (1969) *J. Gen. Physiol.* 54, 306s–326s.
- [11] Fendler, K., Grell, E., Haubs, M. and Bamberg, E. (1985) *EMBO J.* 4, 3079–3085.
- [12] Nakao, M. and Gadsby, D.C. (1986) *Nature* 323, 628–630.
- [13] Raphaeli, A., Richards, D.E. and Karlsh, S.J.D. (1986) *J. Biol. Chem.* 261, 12437–12440.
- [14] Borlinghaus, R., Apell, H.-J. and Läuger, P. (1987) *J. Membr. Biol.* 97, 161–178.
- [15] Mitchell, P. and Moyle, J. (1974) *Biochem. Soc. (Special Publication)* 4, 91–111.
- [16] Stürmer, W., Apell, H.-J., Wuddel, I. and Läuger, P. (1989) *J. Membr. Biol.* 110, 67–86.
- [17] Rakowski, R.F. (1993) *J. Gen. Physiol.* 101, 117–144.
- [18] Gadsby, D.C., Rakowski, R.F. and De Weer, P. (1993) *Science* 260, 100–103.
- [19] Vasilets, L.A. et al. (1993) *Eur. Biophys. J.* 21, 433–443.
- [20] Läuger, P. (1991) in *The Sodium Pump: Structure, Mechanism, and Regulation* (Kaplan, J.H. and De Weer, P., eds.), pp. 303–315, The Rockefeller University Press, New York.
- [21] Stürmer, W., Bühler, R., Apell, H.-J. and Läuger, P. (1991) *J. Membr. Biol.* 121, 163–176.
- [22] Rakowski, R.F., Vasilets, L.A., La Tona, J. and Schwarz, W. (1991) *J. Membr. Biol.* 121, 177–187.

- [23] Bielen, F.V., Glitch, H.G. and Verdonck, F. (1991) *J. Physiol.* 442, 169–189.
- [24] De Weer, P., Gadsby, D.C. and Rakowski, R.F. (1988) *Annu. Rev. Physiol.* 50, 225–241.
- [25] Goldshleger, R., Karlsh, S.J.D., Raphaeli, A. and Stein, W.D. (1987) *J. Physiol.* 387, 331–355.
- [26] Cornelius, F. and Skou, J.C. (1984) *Biochim. Biophys. Acta* 772, 357–373.
- [27] Lindberg, O. and Ernster, L. (1956) *Methods Biochem. Anal.* 3, 1–22.
- [28] Penefsky, H.S. (1979) *Methods Enzymol.* 56, 527–530.
- [29] Peterson, G.L. (1977) *Analyt. Biochem.* 83, 346–356.
- [30] Apell, H.-J. and Berch, B. (1987) *Biochim. Biophys. Acta* 903, 480–494.
- [31] Montal, M. and Mueller, P. (1972) *Proc. Natl. Acad. Sci. USA* 69, 3561–3566.
- [32] Cornelius, F. (1990) *Biochim. Biophys. Acta* 1026, 147–152.
- [33] Andersen, O.S., Feldberg, S., Nakadomari, H., Levy, S. and McLaughlin, S. (1978) *Biophys. J.* 21, 35–70.
- [34] Flewelling, R.F. and Hubbell, W.L. (1986) *Biophys. J.* 49, 531–540.
- [35] Flewelling, R.F. and Hubbell, W.L. (1986) *Biophys. J.* 49, 541–552.
- [36] Ketterer, B., Neumcke, B. and P. Läuger. (1971) *J. Membr. Biol.* 5, 225–245.
- [37] Honig, B.H., Hubbell, W.L. and Flewelling, R.F. (1986) *Annu. Rev. Biophys. Chem.* 15, 163–193.
- [38] Mauzerall, D.C. and Drain, C.M. (1992) *Biophys. J.* 63, 1544–1555.
- [39] Bühler, R., Stürmer, W., Apell, H.-J. and Läuger, P. (1991) *J. Membr. Biol.* 121, 141–161.
- [40] Läuger, P. and Neumcke, B. (1973) in *Membranes* (Eisenman, G., ed.), Vol 2, pp. 1–59, Marcel Dekker, New York.
- [41] Cafiso, D.S. and Hubbell, W.L. (1982) *Biophys. J.* 39, 263–272.
- [42] Cornelius, F. and Skou, J.C. (1988) *Biochim. Biophys. Acta* 944, 223–232.
- [43] Szabo, G. (1974) *Nature* 252, 47–49.
- [44] Franklin, J.C. and Cafiso, D.S. (1993) *Biophys. J.* 65, 289–299.
- [45] Cornelius, F. (1995) *Biochim. Biophys. Acta* 1235, 197–204.
- [46] Beaugé, L.A. and Glynn, I.M. (1979) *J. Physiol.* 289, 17–31.
- [47] Läuger, P. and Apell, H.-J. (1986) *Eur. Biophys. J.* 13, 309–321.
- [48] Läuger, P. and Apell, H.-J. (1988) *Biochim. Biophys. Acta* 944, 451–464.
- [49] Goldshleger, R., Shahak, Y. and Karlsh, S.J.D. (1990) *J. Membr. Biol.* 113, 139–154.
- [50] Bahinski, A., Nakao, M. and Gadsby, D.C. (1988) *Proc. Natl. Acad. Sci. USA* 85, 3412–3416.
- [51] Rakowski, R.F. and Paxson, C.L. (1988) *J. Membr. Biol.* 106, 173–182.
- [52] Bielen, F.V., Glitch, H.G. and Verdonck, F. (1993) *J. Physiol.* 465, 699–714.
- [53] Vasilets, L.A. and Schwarz, W. (1992) *J. Membr. Biol.* 125, 119–132.
- [54] Urry, D.W., Prasad, K.U. and Trapani, T.L. (1982) *Proc. Natl. Acad. Sci. USA* 79, 390–395.
- [55] Ellena, J.F., Dominey, R.N., Archer, S.J., Xu, Z.-C. and Cafiso, D.S. (1987) *Biochemistry* 26, 4584–4592.
- [56] Tsien, R.Y. and Hladky, S.B. (1982) *Biophys. J.* 39, 49–56.
- [57] Klodos, I., and Plesner, L. (1992) *Acta Physiologica Scandinavica* 146, 235–239.
- [58] Läuger, P. (1984) *Biochim. Biophys. Acta* 779, 307–341.
- [59] Apell, H.-J. (1989) *J. Membr. Biol.* 110, 103–114.
- [60] Froehlich, J.P., Hobbs, A.S. and Albers, R.W. (1983) *Curr. Topics Membr. Transp.* 19, 513–535.
- [61] Martin, D.W. and Sachs, J.R. (1991) *J. Gen. Physiol.* 98, 419–426.
- [62] Froehlich, J.P. and Fendler, K. (1991) in *The Sodium Pump: Structure, Mechanism, and Regulation* (Kaplan, J.H. and De Weer, P., eds.), pp. 267–280, The Rockefeller University Press, New York.
- [63] Cornelius, F. (1991) in *The Sodium Pump: Structure, Mechanism, and Regulation* (Kaplan, J.H. and De Weer, P., eds.), pp. 267–280, The Rockefeller University Press, New York.
- [64] Karlsh, S.J.D., Yates, D.W. and Glynn, I.M. (1978) *Biochim. Biophys. Acta* 525, 252–264.
- [65] Nørby, J.G., Klodos, I. and Christiansen, N.O. (1983) *J. Gen. Physiol.* 82, 725–759.
- [66] Yoda, A. and Yoda, S. (1987) *J. Biol. Chem.* 262, 110–115.
- [67] Plesner, I.W. (1986) *Biochem. J.* 239, 175–178.